Supporting Information

Construction of DNA based molecular circuits using normally open and normally closed switches driven by lambda exonuclease

Xin Liu,[a] *Xun Zhang,*[a] *Yao Yao,*[a] *Peijun Shi,*[a] *Chenyi Zeng* [b] and *Qiang Zhang* [*a]

[a] School of Computer Science and Technology, Dalian University of Technology, Dalian 116024, P. R. China

[b] Key Laboratory of Advanced Design and Intelligent Computing, Dalian University, Dalian 116622, China

[*] To whom correspondence should be addressed. Enail: zhangq@dlut.edu.cn

Table of Contents

Table S1 All the DNA sequences used in this work

DNA Oligos	Sequences (from 5′ to 3′)	Length (n.t.)
ss	AGTCACTCCATAACTTACTCCTCAATGTATCATACTCTTAAC	42
5'p strand	PO_4–AGGAGTAAGTTATGGAGTGACT	22
ab	AGCTACTCATACTAGATACACTACTTCAATAACCATCCAATG	42
cd	AGTCACTCCATAACTTACTCCTCAATGTATCATACTCTTAAC	42
PO_4–c*	PO_4–AGGAGTAAGTTATGGAGTGACT	22
b1*a2*a1*ta1d*	GTAGTGTATCTAGTATGAGTAGCTTTTTTTTGCTACTCATACTAGAGTTAAGAGTATGATACATTG	66
da11*	CAATGTATCATACTCTTAACTCTAGT	26
BHQ1–c11	BHQ1–ACTCCATAACTTACTC	16
d1*c1*m–FAM	ATTGAGGAGTAAGTTATGGAGTAGCTAGTTACAGCTTTTTTTTGCTGTAACTAGCT–FAM	56
ed	TCACACTTCCATCATTCTATCACAATGTATCATACTCTTAAC	42
bg	ACTTCAATAACCATCCAATGTAACTC	26
g*b*	GAGTTACATTGGATGGTTATTGAAGT	26
PO_4–i*e1	PO_4–TCACTTCTCTACCAATATCATTTCACACTTCCATCATTCTAT	42
d1*e*	ATTGTGATAGAATGATGGAAGTGTGA	26
PO_4–ib	PO_4–AATGATATTGGTAGAGAAGTGAACTTCAATAACCATCCAATG	42
CY5–i11*	CY5–CTTCTCTACCAATATC	16
e11*i1n–BHQ3	TGAAATGATATTGGTAGAGAAGAGCTAGTTACAGCTTTTTTTTGCTGTAACTAGCT–BHQ3	56
a11d*	ACTAGAGTTAAGAGTATGATACATTG	26
PO_4–e*	PO_4–TGATAGAATGATGGAAGTGTGA	22
e1h	TCACACTTCCATCATTCTATCACACTCT	28
h*e1*	AGAGTGTGATAGAATGATGGAAGTGTGA	28
PO_4–i*e1x (x=3)	PO_4–TCACTTCTCTACCAATATCATTTCACACTTCCATCATTCTATCACA	46
PO_4–i*e1x (x=2)	PO_4–TCACTTCTCTACCAATATCATTTCACACTTCCATCATTCTATCAC	45
PO_4–i*e1x (x=1)	PO_4–TCACTTCTCTACCAATATCATTTCACACTTCCATCATTCTATCA	44
PO_4–i*e1x (x=0)	PO_4–TCACTTCTCTACCAATATCATTTCACACTTCCATCATTCTATC	43

PO4–ie1x (x=3)	PO4–AATGATATTGGTAGAGAAGTGATCACACTTCCATCATTCTATCACA	46
PO4–ie1x (x=2)	PO4–AATGATATTGGTAGAGAAGTGATCACACTTCCATCATTCTATCAC	45
PO4–ie1x (x=1)	PO4–AATGATATTGGTAGAGAAGTGATCACACTTCCATCATTCTATCA	44
PO4–ie1x (x=0)	PO4–AATGATATTGGTAGAGAAGTGATCACACTTCCATCATTCTATC	43
PO4–a*	PO4–AGTGTATCTAGTATGAGTAGCT	22
FAM–a1pa*–BHQ1	FAM–TCATACTAGATACACATTTTTTAGTGTATCTAGTATGAGTAGCT–BHQ1	44
ROX–c1qc*–BHQ2	ROX–TCCATAACTTACTCCATTTTTTAGGAGTAAGTTATGGAGTGACT–BHQ2	44
jo	CAATCACCAATTCAAACTTCCACTTA	26
jk	CAATCACCAATTCAAACTTCTTCAAC	26
d1fj	CAATACTTCCATCATTCTATCACAATCACCAATTCAAACTTC	42
o*j*	TAAGTGGAAGTTTGAATTGGTGATTG	26
PO4–f*d1*	PO4–TGATAGAATGATGGAAGTATTG	22
k*j*	GTTGAAGAAGTTTGAATTGGTGATTG	26
PO4–cd1f1	PO4–AGTCACTCCATAACTTACTCCTCAATACTTCCATCATTCTAT	42
j1f*d1*	ATTGTGATAGAATGATGGAAGTATTG	26
PO4–c*b	PO4–AGGAGTAAGTTATGGAGTGACTACTTCAATAACCATCCAATG	42
i1*e11b	CTTCTCTACCAATATCATTTCAACTTCAATAACCATCCAATG	42
i1*e11d	CTTCTCTACCAATATCATTTCACAATGTATCATACTCTTAAC	42
PO4–e11*i1	PO4–TGAAATGATATTGGTAGAGAAG	22

The hydrolysis experiment of NO 2 is conducted to verify the feasibility of the blocking strategy, as shown in Figure S1. The hydrolysis reaction under the concentration of λ exo and incubation time is explored. It can be observed that NO 2 is stable irrespective of whether the reaction time or the concentration of the enzyme is increased.

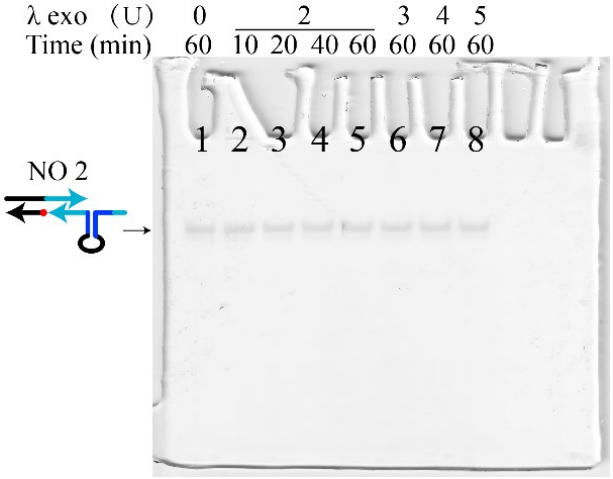

Figure S1. Hydrolysis experiment of NO 2 at the background of λ exo. NO 2 without λ exo for 60 min (lane 1); the incubation of annealed NO 2 at 2U λ exo for 10–60 min (lanes 2–5); the incubation of NO 2 at the background of 3U (lane 6), 4U (lane 7), and 5U (lane 8) λ exo for 60 min.

In Fig. 1E, the band of Indicator 1 in lane 6 is slightly lower than the same band in lane 7, the reason of which is analyzed by a PAGE experiment, as shown in Fig. S2. It can be found that Indicator 1 has a good resistance to the hydrolysis of λ exo for the comparison of lanes 2 and 3, and the band of Indicator 1' offset from Indicator 1 can be obtained in lanes 1 and 5. According to the bands of Indicator 1' in lanes 1 and 5, the structural differences between Indicator 1 and Indicator 1' are caused by hydrolysis, and it can be inferred that Indicator 1 and Indicator 1' are difference in base numbers. Therefore, we can analyze the reaction process in lane 5 that generates the same band of Indicator 1' to infer the cause of Indicator 1' instead of analyzing it in the complex lane 1. In lane 5, there are only two types of substrates in lane 5, which are NO 2-2 and Reporter 1. Some researchers found that the relative kcat for 5' ends decreases in the order 5′ recessed > blunt >> 5' overhang,[1] and showed a DNA duplex with a 5' non-phosphorylated, two-nucleotide (2-nt) protruding end can be digested by λ exo with very high efficiency.[2] These researches confirm the possibility of hydrolysis of the 5' blunt in NO 2-2 instead of the 5' overhang in Reporter 1. In addition, Indicator 1 cannot be hydrolyzed in lane 3. Supported by these evidences, we can infer that the hydrolysis of the 5' blunt in NO 2, NO 2-1 or NO 2-2 results in the structural differences between Indicator 1 and Indicator 1'. In addition, there is no leakage in the mixture of NO 2-2 and Reporter 1 for the comparing of lanes 6 and 7.

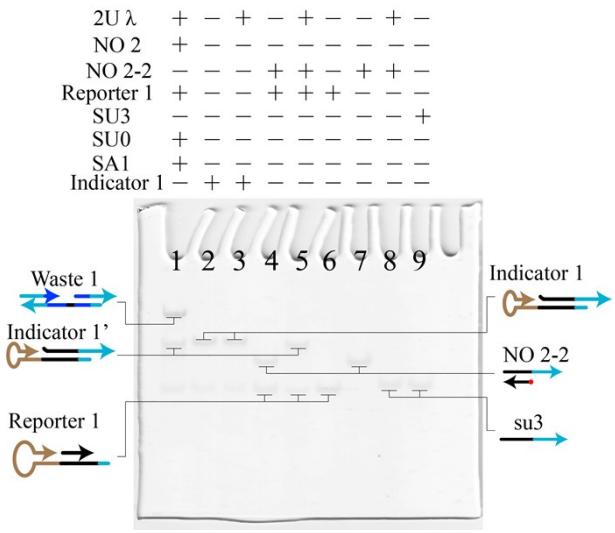

Figure S2. Comparison of Indicator 1 under different hydrolysis conditions. The mixture of Reporter 1 and NO 2 with the addition of SU0 and SA1 at 2U λ exo (lane 1); Indicator 1 (lane 2); Indicator 1 with 2U λ exo (lane 3); The mixture of Reporter 1 and NO 2-2 (lane 4); The mixture of Reporter 1 and NO 2-2 added with NO 2-2 at 2U λ exo (lane 5); Reporter 1 without c11* (lane 6); NO 2-2 (lane 7); NO 2-2 with 2U λ exo (lane 8); SU3 (lane 9).

The outputs of NO 2 with the addition of SU0 and SA1 are monitored at different concentration of λ exo, as shown in Figure S3. It is obvious that NO 2 cannot be triggered without λ exo, and the reaction rates become fast with the increase of enzyme concentration.

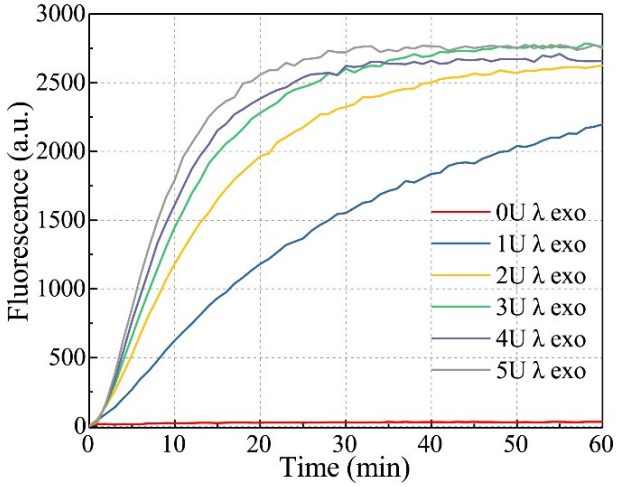

Figure S3. Real-time fluorescence monitoring of NO switch at different concentration of λ exo.

The hydrolysis experiment of NC 0 is conducted in Figure S4. The result is similar to the gel in Figure S1, and the blocked structure NC 0 is stable no matter whether the reaction time or the concentration of enzyme is increased.

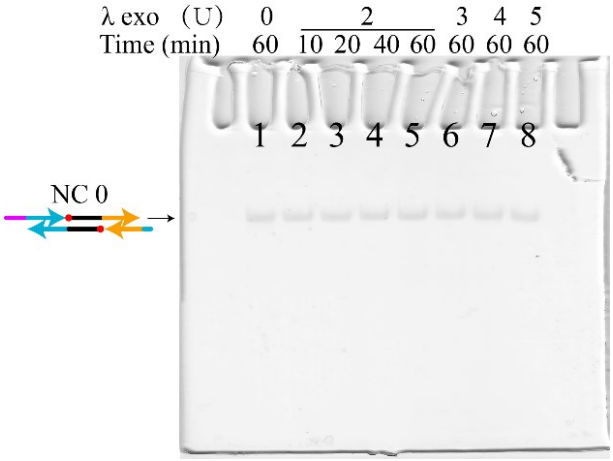

Figure S4. Hydrolysis experiment of NC 0 at the background of λ exo. NC 0 without λ exo (lane 1); the incubation of NC 0 at the background of 2U λ exo for 10–60 min (lanes 2–5); the incubation of NC 0 at 3U (lane 6), 4U (lane 7), and 5U (lane 8) λ exo for 60 min.

The outputs of NC 0 with the addition of SU21 are monitored at different concentration of λ exo, as shown in Figure S5. Similarly, NC 0 cannot be triggered without λ exo, and the reaction rates become fast with the increase of enzyme concentration.

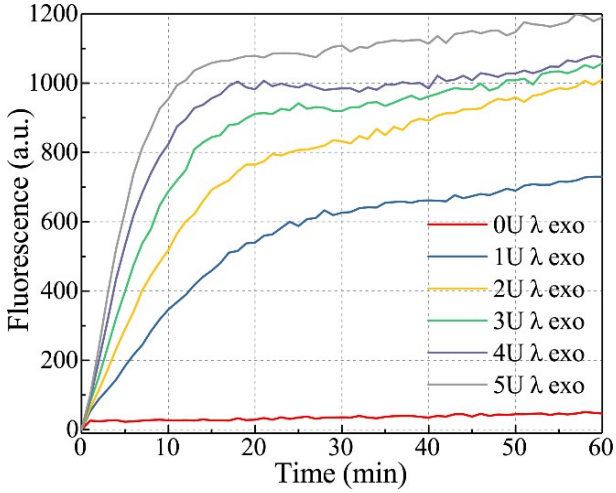

Figure S5. Real-time fluorescence monitoring of NC switch at different concentration of λ exo.

The feasibility of cascaded NO and NC switches is verified in Figure S6. Indicator 2 is generated after the addition of SA1 (lane 9), but the band of Indicator 2 cannot be found with the addition of SA1 and SA0 in lane 10.

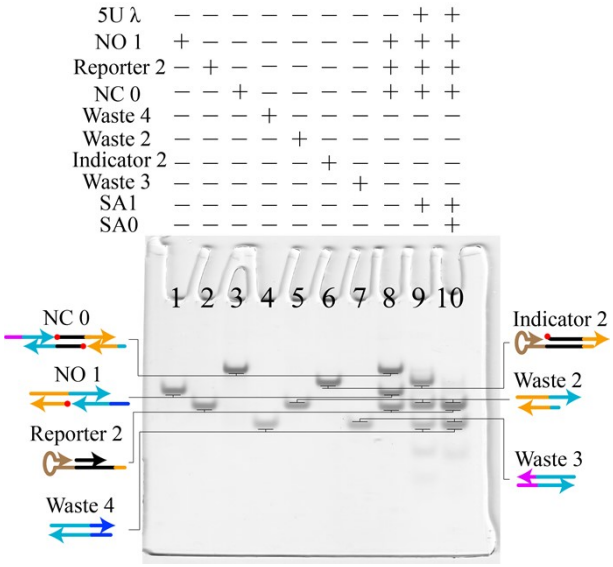

Figure S6. PAGE gel of cascaded NO and NC switches. NO 1 (lane 1); Reporter 2 (lane 2); NC 0 (lane 3); Waste 4 (lane 4); Waste 2 (lane 5); Indicator 2 (lane 6); Waste 3 (lane 7); mixture of NC 0, NO 1, and Reporter 2 without λ exo (lane 8); cascaded NO 1, NC 0, and Reporter 2 with the addition of SA1 (lane 9) or with the presence of SA1 and SA0 at 5U λ exo.

Cg-NC is designed as the control group of time-delay relay (Figure S7) to simulate Td-NC without left toeholds by the method of blocking the left of Cg-NC with an unrelated g*b*. If the left toeholds of h*-x in Td-NC are reduced to 0 using the same strategy of Figure 4, the hydrolyzed left product would be hybridized with TIN, and the consumed TIN will reduce the final output, which is unfavorable to our experiment. Whereas in Figure S7, since TIN can only be responded by the right side of Cg-NC, the leakage caused by the left side of Cg-NC can be avoided. In addition, the product g*b * after the hydrolysis of Cg-NC-1 cannot be hybridized with TIN, which will not affect the input or output signals.

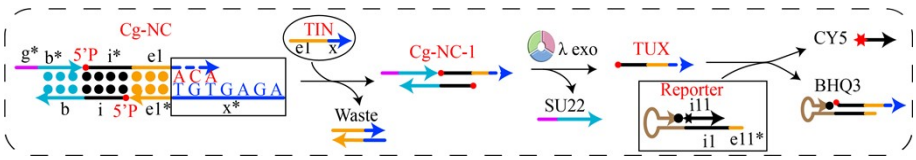

Figure S7. Schematic diagram of the control group of time-delay relay.

The reaction route II in Figure 4A is analyzed independently, as shown in Figure S8A. Td-NC 2 is annealed by all the combinations of TDX and TUX (x = 3, 2, 1, or 0). λ exo as input is added to the mixture of Td-NC 2 and Reporter, the reaction of which is divided into four idealized reaction routes. In route i, Td-NC 2 directly undergoes a strand displacement reaction with Reporter to produce the fluorescence signal without weakening. In route ii, λ exo hydrolyzes Td-NC 2 from the 5' recessed end of TDX to produce TUX, which displaces CY5-i11* from Reporter to output the unabated fluorescence signal. Opposite to route ii, λ exo hydrolyzes Td-NC 2 from the 5' recessed end of TUX to generate TDX unrelated to Reporter in route iii, which is unable to generate or reduce the fluorescence signal.

However, the decrease of fluorescence occurs in route iv. λ exo hydrolyzes 5' recessed end from both sides of Td-NC 2, the phenomenon of which is similar to Figure 1A. As the hybridized domain of i-i* decreases, the hydrolyzed product of Td-NC 2 disassembles into TUX' and TDX', which is a reversible reaction. Since the length of ix* gradually decreases under the hydrolysis of λ exo, TUX' displaces CY5-i11* from Reporter to produce the fluorescence signal and Indicator 3, and the length of ix* is not sufficient to cover the gap domain of Indicator 3, the structure of which is unstable and leads a strand displacement reaction between CY5-i11* and Indicator 3 to reproduce Reporter, causing the decrease of fluorescence, as shown in Figure S8B. The results of fluorescence experiments reveal the reason for the fluorescence reduction in Figure 4B–E.

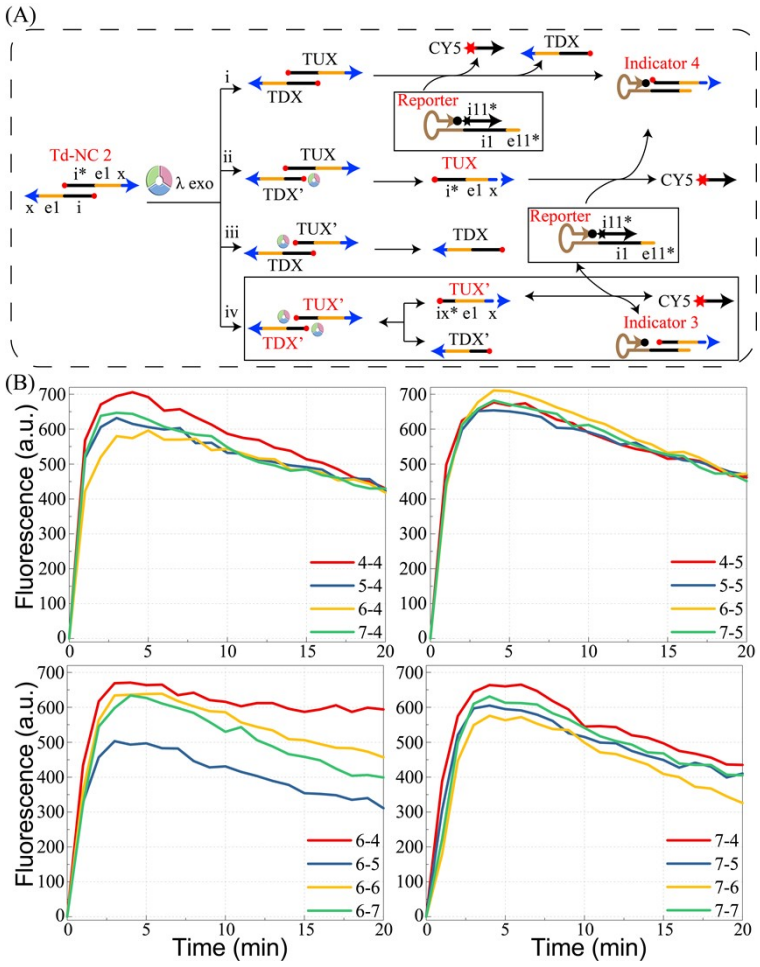

Figure S8. Analysis of reaction route II in time-delay relay.

Td-NC with different toehold combinations is explored to obtain the quantitative outputs, as shown in Figure S9. All the values are normalized by the maximum fluorescence in Figure 4F.

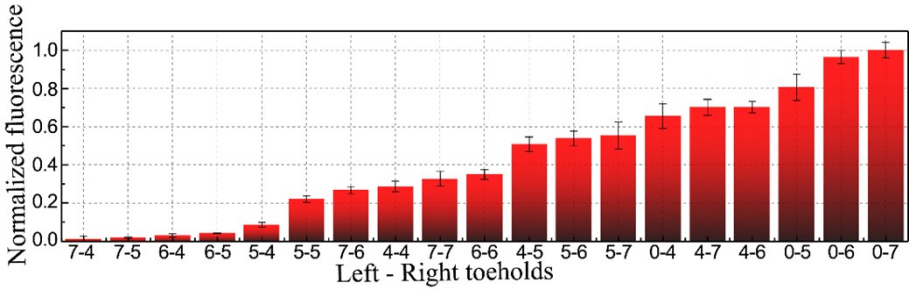

Figure S9. Quantitative outputs of time-delay relay.

The schematic diagram of digital square circuit is shown in Figure S10, which is constructed by the basic forms of NO and NC switches. Considering the loss of signal during transmission, s0, s2, and s3 are set to 10 pmol, and all the switch substrates are 20 pmol. The inputs are twice the amount of corresponding switch substrates, and both SA0 and SA1 are 80 pmol. 10U λ exo is added to the solution to drive the square operation.

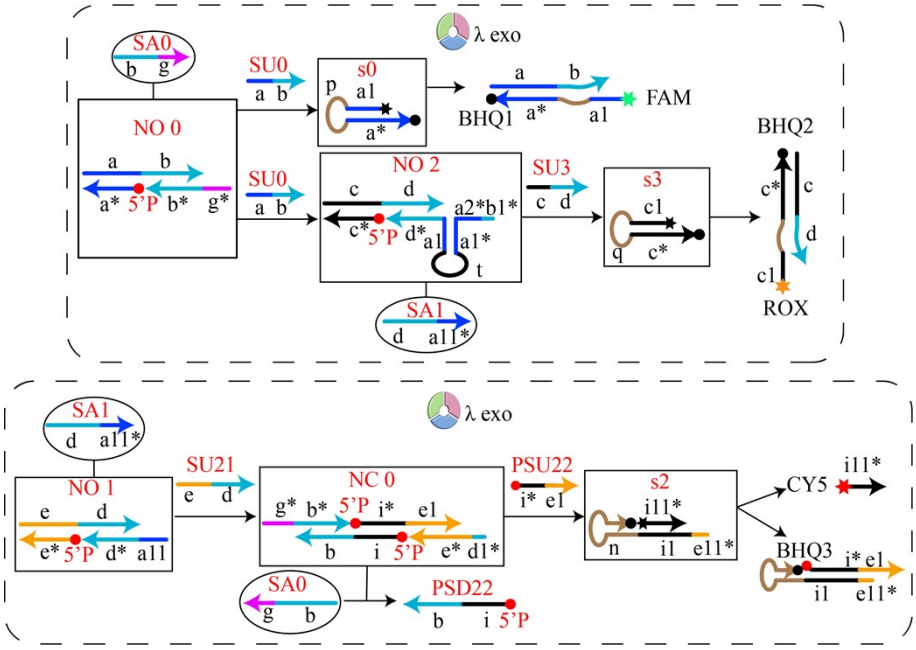

Figure S10. Schematic diagram of square circuit.

The hydrolysis of s0 (Figure S10) under different concentration of λ exo is explored in Figure S11. As one of the reporters, the 5' end of s0 is modified with FAM, which causes the hydrolysis reaction to obtain the outputs under different concentration of λ exo. It can be found that the increase of enzyme concentration accelerates the hydrolysis reaction.

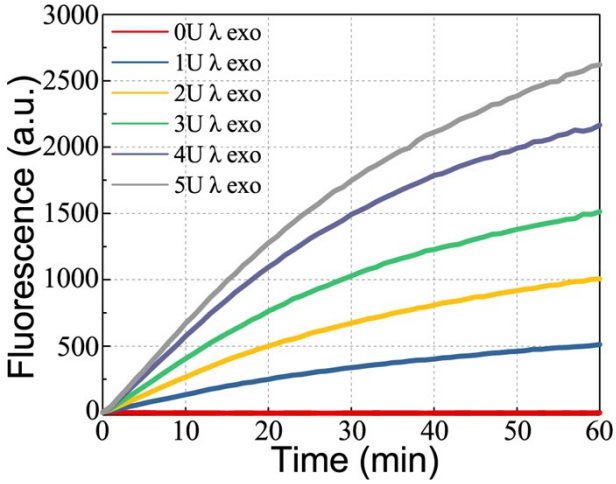

Figure S11. Real-time fluorescence monitoring of leakage under different concentration of λ exo.

The schematic diagram of digital square circuit is shown in Figure S12. Similarly, r0, r1 are 10 pmol, and all the switch substrates are 20 pmol. The inputs RA0, RA1, RA2, and RA3 are 40 pmol, 40 pmol, 120 pmol, and 80 pmol, respectively. 10U λ exo is added to drive the digital square operation.

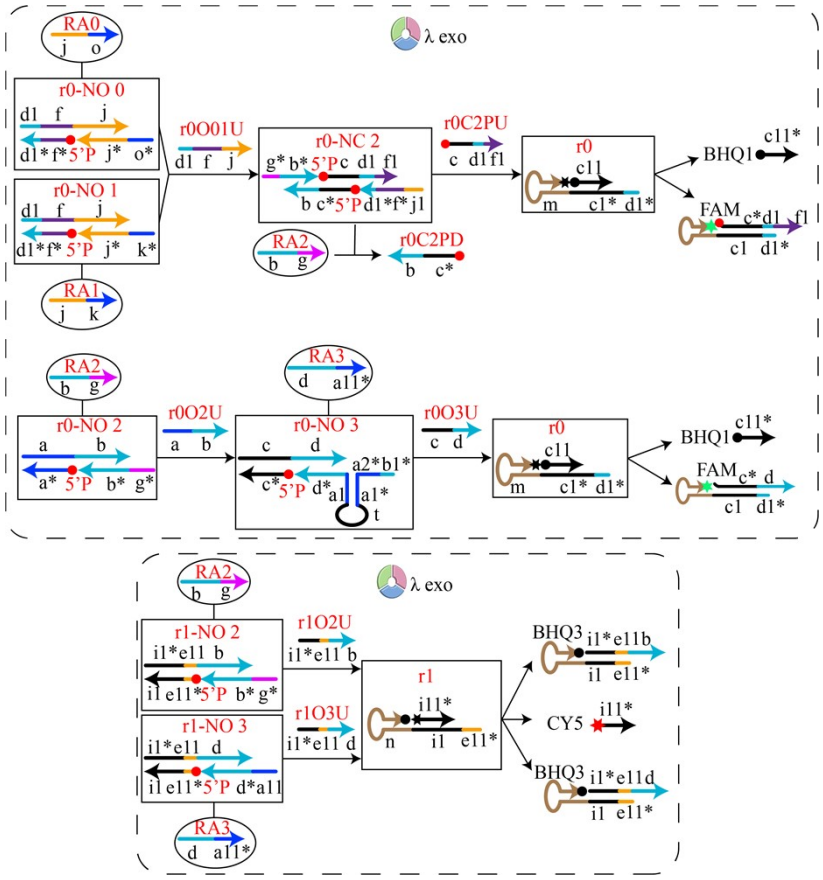

Figure S12. Schematic diagram of square root circuit.

The outputs of digital square root circuit with all possible inputs are explored in Figure S13.

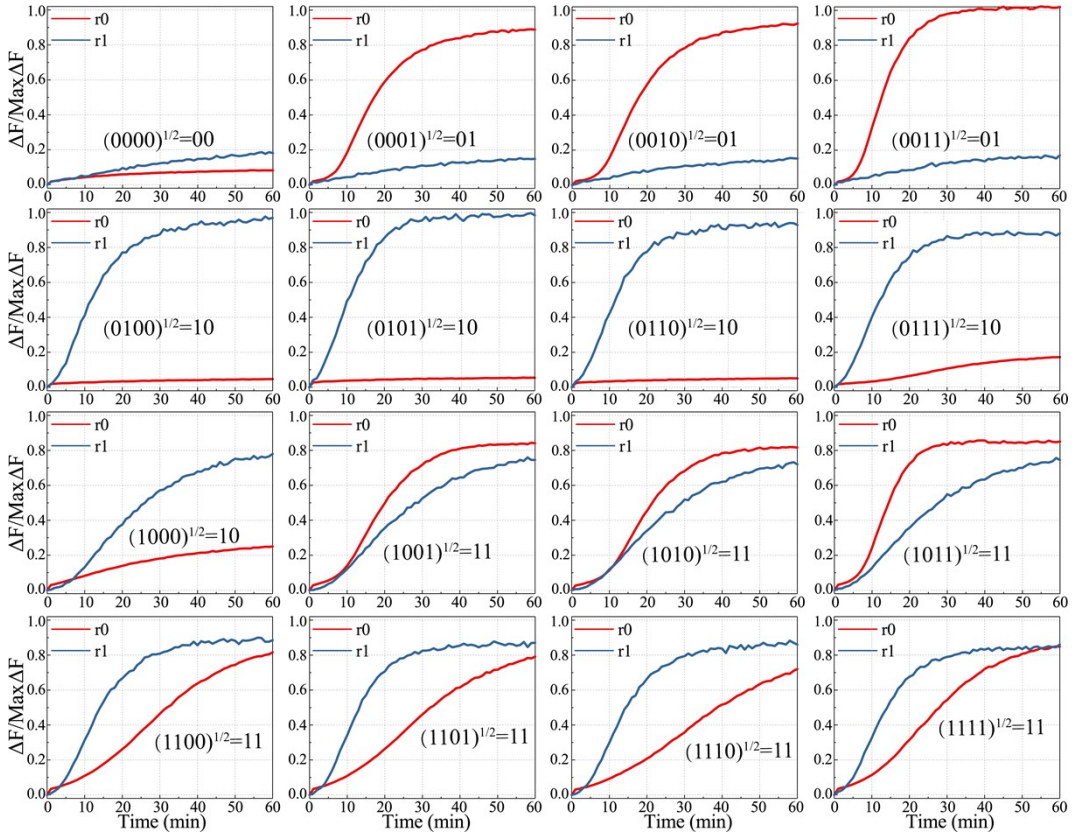

Figure S13. Real-time fluorescence monitoring of square root operation with 16 combinations of inputs.

References

1. P. G. Mitsis and J. G. Kwagh, *Nucleic Acids Res.*, 1999, **27**, 3057–3063.
2. T. Wu, Y. Yang, W. Chen, J. Wang, Z. Yang, S. Wang, X. Xiao, M. Li and M. Zhao, *Nucleic Acids Res.*, 2018, **46**, 3119–3129.